ISSN: 0975-8585

Research Journal of Pharmaceutical, Biological and Chemical Sciences

Evolution of the Film Structure in the Various Evaporation Processes.

Kameneva AL*.

Perm National Research Polytechnic University, Department of Innovative Engineering Technology, Komsomol'skii pr. 29, Perm, 614990, Russia.

ABSTRACT

The work analyzed structural zone models (SZM) of films produced by electron beam evaporation, thermal evaporation, anodic and cathodic arc evaporation. The structural evolution of films in SZM is studied as a function of temperature, technological and physical parameters of the deposition process: substrate temperature, migration of grain boundaries, film pollution level, impurities concentration, which is related to the ratio of intensities of impurity and metal input flow, Ar and N gas mixture pressure. Zone 1, compared to existing SZM, can be presented as an independent SZM. In the low-temperature range $0.15<Ts/Tm<0.23$ (Ts/Tm is the ratio of the substrate temperature (Ts) to the melting point of the deposited film (Tm) material in Kelvin degrees), the structure evolution of three-component thin polycrystalline films Ti1–xAlxN and TixZr1–xN is studied at Tm ~ 4000 K. Formation stages of Ti1–xAlxN and TixZr1–xN films during the cathodic arc evaporation are determined, and SZM of films as a function of Ts/Tm and film heating rate (Vheat.) is developed. It is shown that the increase of adatoms mobility, decrease of crystallites disorientation, their preferred orientation and formation of solid nanostructured homogenous films to the forming direction are determined by the appropriate film heating rate in its deposition Vheat.= 6 K/min.

Keywords: structural zone models, polycrystalline films, the evolution of structure, temperature, technological and physical parameters of the deposition process, different methods of evaporation.

Corresponding author

ISSN: 0975-8585

INTRODUCTION

It is known that the possibility to produce films with a given stable structure is limited. The current composition of polycrystalline film, shape, size, crystal-lattice orientation of the polycrystalline phase and its mutual distribution to the amorphous phase are unstable. A growing attention of many scientific schools worldwide is paid to the issue how to manage and stabilize the structure of polycrystalline film during its deposition. Scientific trials are aimed at the study of regularities of how technological and temperature deposition parameters affect the evolution of the structure of polycrystalline films and development of new methods for a full description of phenomena, which are responsible for the development of different film structures. The development of structure zone models (SZM) is one of those methods for the study of how temperature and process deposition parameters effect mutually on film structural changes.

This article analyzed SZM of polycrystalline films produced by electron beam evaporation, thermal evaporation, anodic and cathodic arc evaporation. The film structure evolution in SZM is studied depending on temperature, technological and physical deposition parameters: substrate temperature, migration of grain boundaries, film pollution level, impurities concentration, which is related to the ratio of intensities of impurity and metal input flow, Ar and N_2 gas mixture pressure. The author of the paper determined that the evolution of structure and velocity of film structure formation, complementary to the substrate temperature, is affected by its heating rate in the deposition.

STRUCTURAL ZONE MODELS OF FILMS PREPARED BY THE ELECTRON-BEAM EVAPORATION

In order to describe the evolution of the structure and film formation, in 1969 Movchan and Demchishin have developed a structural zone model (SZM) [1], which sets a regularity of structuring of thick single-phase films Ni, Ti, W, Al_2O_3 and ZrO_2 (to 2 mm***) using the electron-beam evaporation in the temperature range*** (0.22…0.3)<T_s/T_m<(0.45…0.5) (the ratio of the substrate temperature (T_s) to the melting point of the deposited film (T_m) material in Kelvin degrees). It has been first shown that the film structure change was due to an increase of the ratio T_s/T_m, to the specified intervals of which at least three zones with qualitatively different structures (Fig. 1) correspond. Under temperature conditions that relate to the zone 1, T_s/T_m < 0.22…0.3, the film surface has a specific globular dome-shaped structure, the hemisphere diameter of which increases with growth of T_s/T_m [1]. Very small crystallites were found to form originally on the substrate surface, and then they form at an angle to the film surface if there are microroughnesses [2, 3], with the increase of T_s they grow in size with simultaneous micropores formation [4], and if there are no microroughnesses on the film surface, a columnar structure forms [5]. A high density of irregularities of the lattice and pores on the grain boundary is typical for the zone 1. At T_s = 0.3 T_m, which is, in particular, 663 and 573 K for films Ti and Ni, respectively [6], a smooth transition occurs to the zone 2 with a flat finish. A small temperature increase T_s is accompanied with a globular structure coarsening of the zone 1, which gradually comes to a columnar one, specific for the zone 2. The width of columnar crystallites grows with the increase of T_s, and their slope is related to the flow direction of film-forming particles. A peculiarity of the zone 2 is the presence of well-defined intercrystalline boundaries due to processes of the "surface" recrystallization [1, 4, 7-8]. A columnar film structure is observed at T_s/T_m < (0.45…0.5)***. At peak temperatures of the zone*** 2 and intensification of the surface diffusion, the grain size increases and gets comparable to the film thickness, there is a faceting on the grain surface. An equiaxial film structure, which corresponds to the zone 3 T_s/T_m>(0.45…0.5), forms as a result of the secondary recrystallization of columnar crystallites [1, 3, 5]. The temperature threshold T_s/T_m=(0.45…0.5) between zones 2 and 3 is unstable and depends on impurities in the film, preparation of the substrate surface and film deposition rate [3, 8]. In the contribution [3], the peak value T_s/T_m is increased to 0.70. In the zone 3, the surface of metal films is shine with a specific polyhedral structure.

Grovenor etc. [9] showed that in models [1, 10, 11] the effect of the surface diffusion and recrystallization on the grain film structure is presented not clearly enough. In the first SZM [1], the formation of different structures is explained by the surface energy behavior, which controls the recrystallization, on T_s/T_m, and in Grovenor's SZM (Fig. 2), for a certain deposition mode by electron-beam evaporation, – by the grain structure behavior on T_s/T_m and migration of grain boundaries assumed to be a predominant parameter [9, 12-14], on grounds that both the mobility and activation energy depend on their crystallography and film contamination level in the sliding of grain boundaries [9]. The key reason why Grovenor had improved SZM

was a gradual transition between zones 1 and 2 with large grains having the bimodal grain-size distribution, and which was found in the low-temperature range T_s/T_m [15].

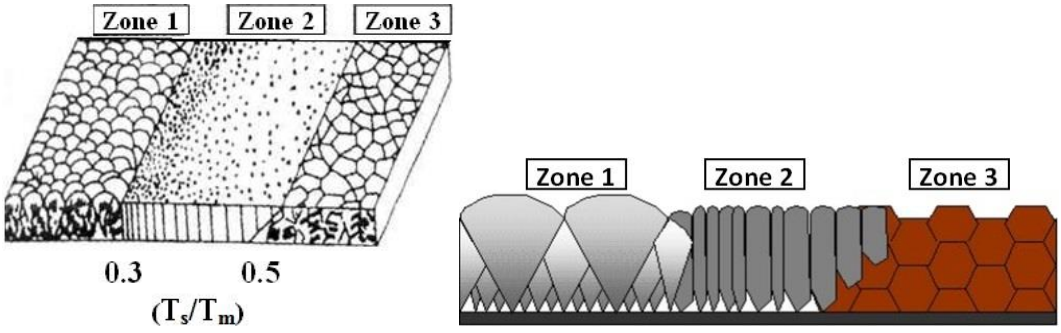

Figure 1: Model of Movchan and Demchishin (1969): electron-beam evaporation

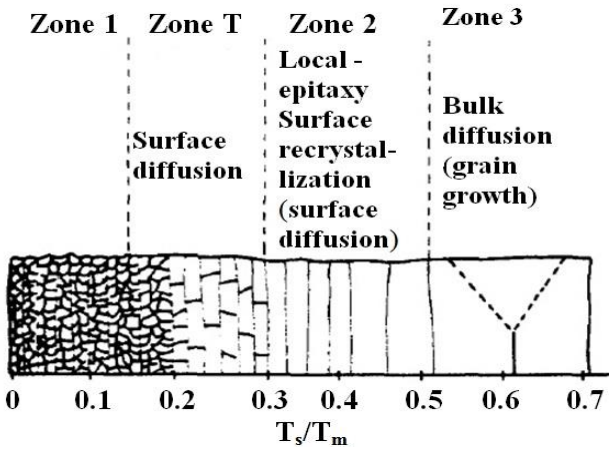

Figure 2: Model of Grovenor (1984): electron-beam evaporation

The structural change is linked by Grovenor etc. with the dual film deposition process: forming of grains and granulated epitaxy. The researchers established the regularities of change in some structural parameters under the temporary relation T_s/T_m, explaining the change in grain size and morphology of the film during the formation of grains with mobile boundaries.

The Grovenor's model, which generalizes existing SZM and allows to classify the structure of both thick and thin metal films with interpreting its development, is used not often enough for the analysis in academic and applied research [15-18].

THERMAL EVAPORATION

Further systematic experiments were performed by Barna and Adamik to clarify details in correlation between the structure, temperature, deposition parameters and to explore reasons of distinct film morphology obtained by reactive deposition in different experiments at the same temperature [19]. Specifically for the investigation of impurities effect on the film structure development, the impurity concentration was varied by changing the ratio of intensities of impurity and metal input flow. Oxygen and aluminum were used as the model system [20]. The choice of O and Al as impurity and metal is based on the low solubility of oxygen in aluminum; its deposition on the surface and grain boundaries as two-dimensional (2D) oxide layers (oxide thin phases), multiply decreasing the surface of Al and movement of grain boundaries, changing all processes of film forming by limiting the coarsening grains in film joining and forming (Fig. 3, a, 1), as well as on the periodic interruption of epitaxial forming of singular crystallites, segregation processes and the renucleation of generation centers of nanocrystallite grains separated with a thin amorphous phase (here,

AlO_x) [20]. Changes in the structure and crystal-lattice orientation of the film as a function of the increasing oxygen concentration are confirmed with schemes on Figure 3, a [21].

The oxygen incorporates in grain boundaries and continues to accumulate during their movement, eventually suppressing the grain formation due to the «impurity diffusion», if the intensity ratio of oxygen and aluminum input flow, $I_O/I_{Al} \approx 10^{-3}$, is low. The structure obtained remains in the zone 2 with columns distributed over the whole film, but having a less preferred orientation and smaller grain size (Fig. 3, *a*, 2).

With the insignificantly greater oxygen concentration level (zone T, $I_O/I_{Al} \approx 10^{-2}$), the grain coarsening in the joining is strongly suppressed resulting in an irregular grain orientation. The continuing concurrent forming is affected by the crystallographic anisotropy [20] (the oxygen is deposited the most quickly on 111 surfaces) (Fig. 3, *a*, 3).

With an increased oxygen concentration (zone 3, $I_O/I_{Al} \approx 0{,}1\ldots1$), the oxide layer is fully covered with islands having crystal-lattice orientation 111, 001, 110, and there is no coarsening in the joining, then the film continues to form through the renucleation.

From [1] it is known that the film is composed of 3D equiaxial (globular) grains with a random orientation and corresponds to the zone 3 (Fig. 3, *a*, 4). With increasing the oxygen concentration, the grain formation is decreased and may reach the nanosized level. An important side effect of the renucleation through the forming of film nanograins – surface faces do not cover individual columns, and there is an associated shading effect, thus, nanophase films are actually smoother and, hence, denser. Oxide phase also suppress the movement of grain boundaries, preventing the coarsening in quantities, and increase the thermostability.

In the event of the further oxygen concentration increase ($I_O/I_{Al} \approx 2\ldots5$), the effect of oxide and metal phase inverted: the oxide phase generates first nuclei, while Al is deposited on the surface, and 3D islands are formed [20]. Films obtained are composed of metal grains distributed through the oxide matrix (Fig. 3, *a*, 5) [20]. Such composite films composed of the matrix with a low thermal conductivity and metal impurities are the basic class of ceramics-metal films with various applications.

With very high oxygen intensities ($I_O/I_{Al} >> 1$), the films are fully composed of Al oxide, which is amorphous under the ambient forming temperature. Values T_s, exceeding 800 °C, are shown for the formation of chemically and mechanically stable *k*- and α-phases of Al oxide. The researchers tried to obtain a hard crystal Al oxide using the ion-assisted deposition under temperatures below 500 °C [22].

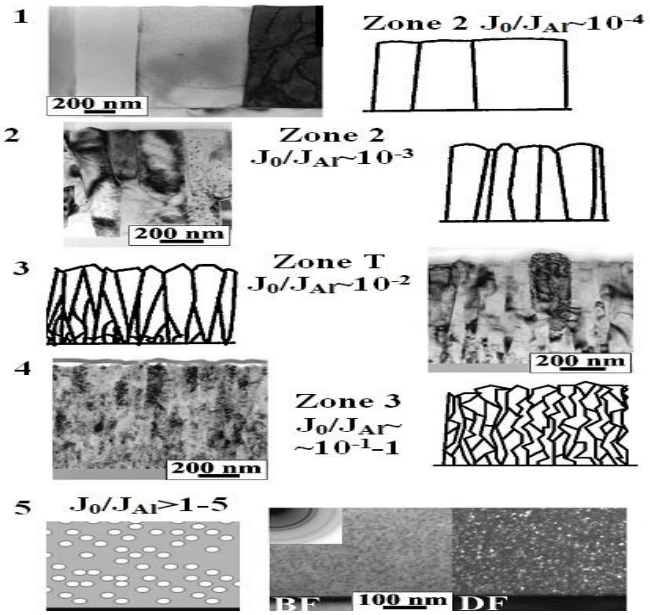

Figure 3: Model of Barna and Adamik (1998): thermal evaporation

ISSN: 0975-8585

ANODICARC EVAPORATION [23]

Due to concentration of pure Cu plazma, compact homogenous Cu films form with purity more than 99.995% and apparent density, regardless of condensation parameters. The relation of microstructure to the energy of ions E_i, the flux ionization X and T_s/T_m may be presented as a SZM (Fig. 4), different from those used for evaporation [1] or sputtering [5]. Zone 1 does not exist in Mausbach's model.

At T_s/T_m<0.3 and average ion energy per atom <E_i>over 1 eV/atom, the zone 1 in Mausbach's model is replaced by the zone M with a dense metastable structure. The grain growth in zone M is athermic with an average grain size of about 1 μm. By increasing <E_i>, the regrowth time goes up. The film metastability is related to point defects in the film structure that diffuse at room temperature due to their low activation energy. At constant T_s/T_m and growing E_i and X, the grain growth decreases.

At T_s/T_m>0.3 and high X, the grain growth is much less than in zone M. However, under such conditions, a thermally activated grain growth is found with an activation energy 0.1-0.29 eV for X = 2% and X = 27%. The lowest relation of grain to E_i exists. In this temperature area, metastability disappears due to the high mobility of point defects produced. Immediately upon the condensation, the film is in stable crystalline state.

At T_s/T_m=0.45…0.5, compared to known SZM, no boundary is found between zones 2 and 3. A more or less continuous transition between zones is determined. Mausbach designated this area as «zone K». Figure 4 shows SZM of pure Cu plasma condensation, as function E_i, X and T_s/T_m.

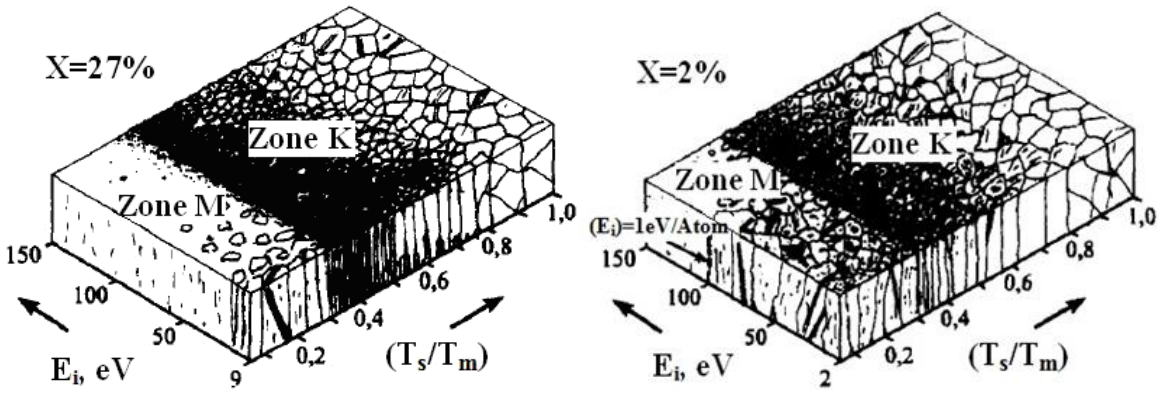

Fiure 4: Model of Mausbach (1995): anodic arc evaporation

CATHODIC ARC EVAPORATION

Three-component films $Ti_{1-x}Al_xN$ and $Ti_xZr_{1-x}N$ were produced in the temperature range T_s/T_m =0.15…0.23, which belongs to the zone 1. Compared to previous models, it is determined that in this zone 1, the increase of pressure (P) gas mixture of Ar and N from 0.5 Pa to 1.0 Pa is results in growth of a heating rate of the film during its deposition ($V_{heat.}$) from 1.9 K/min to 4 K/min, and the increase of substrate bias voltage (U_{bias}) from 200 V to 280 V – in a further increase $V_{heat.}$ to 6 K/min. Due to the fact of the structure evolution, three-component films $Ti_{1-x}Al_xN$ and $Ti_xZr_{1-x}N$ were studied as a function of four parameters: T_s/T_m, $V_{heat.}$, P and U_{bias}.

T_s/T_m and $V_{heat.}$ are determined for each formation stage of polycrystalline films in zone 1 [24–30]:

(1) – *Globular stage* (T_s/T_m = 0.154...0.171, $V_{heat.}$= 1.9 K/min): formation and combination of isometric structures – globules. At this stage, any orientation of boundary areas is fully absent in the film (Fig. 5, a).

(2) –*{100} facets on globules* (T_s/T_m = 0.171...0.179, $V_{heat.}$ = 2.2 K/min). At initial stages, primary polycrystalline buildups originate on globules as seed crystallites with {100} facets (Fig. 5, b), then many small {100} facets form on globules perpendicular to the substrate surface (Fig. 5, c).

ISSN: 0975-8585

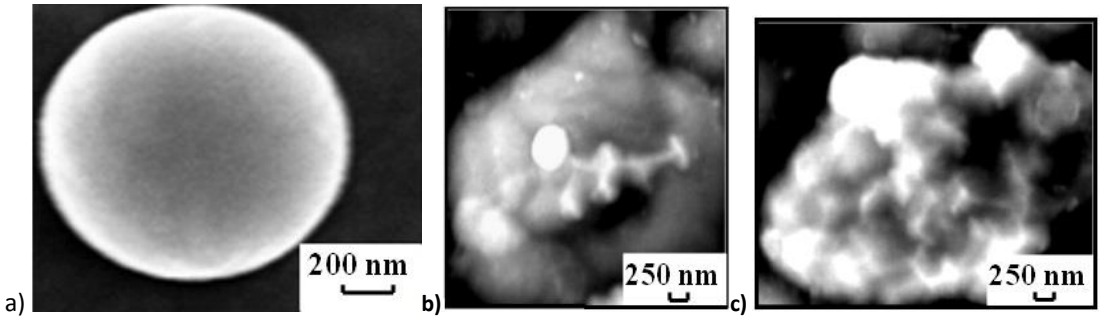

Figure 5: Micrograph of the surface of $Ti_{1-x}Al_xN$ film at the stage of: formation and combination of globules (a), formation of many small {100} facets on globules (b, c)

(3) - Nucleation (Fig. 6, *a*) *and intergrowth of seeds of the polycrystalline component of $Ti_{1-x}Al_xN$ film* (Fig. 6, *b*) (T_s/T_m = 0.179…0.187, $V_{heat.}$= 3.5 K/min). Due to the intergrowth of pyramid-like crystallites with pseudo-hexagonal supports, they grow in size from 200 to 700 nm (Fig. 6, *c*). This is explained by the texturizing of crystallites on further stages of $Ti_{1-x}Al_xN$ film formation.

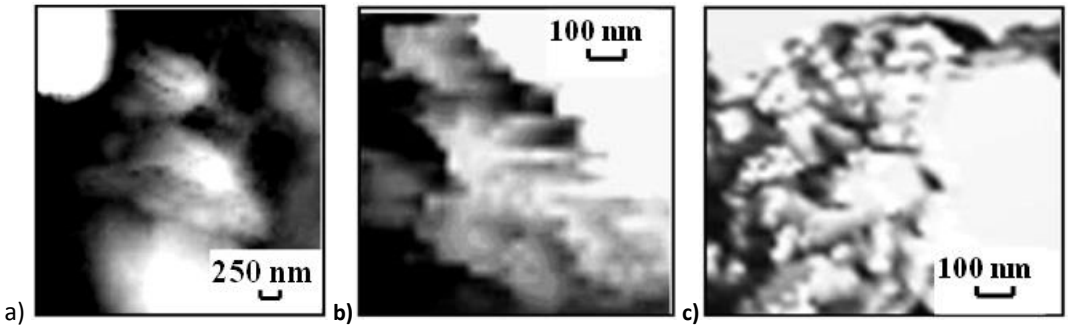

Figure 6: Micrograph of the surface of $Ti_{1-x}Al_xN$ film at the stage of: nucleation (*a*) and intergrowth of seeds of the polycrystalline component of $Ti_{1-x}Al_xN$ film (*b*). Crystallites growth (*c*)

(4) –Formation stage of the primary axial<100>texture, geometric selection. At T_s/T_m = 0.187…0.205 and $V_{heat.}$= 4.0 K/min, the density of active nucleation centers changes, the preferred direction of crystal-lattice orientation of $Ti_{1-x}Al_xN$ film phases also changes, as well as the volume fraction of three-component $Ti_3Al_2N_2$ phase increases in maximum (Fig. 7). The relatively high energy of boundaries twinning in Al excludes the formation of multiply twinned crystallites in the vacuum condensation. However, when the energy of twinning boundaries decreases due to the three-component nitride $Ti_3Al_2N_2$, twinned {100} crystallites form on X-ray amorphous globules, whose facets are almost parallel to the substrate surface (Fig. 7, *a*). If $Ti_{1-x}Al_xN$ film has a certain thickness, the primary axial <100> texture stops forming and multiple axil angles form due to the twinning on the surface of {100} plates. A single twinning observed on {100} facets (Fig. 7, b) provides an explanation for the formation of the secondary cone <110> texture on the axial <100> texture (Fig. 7, c) and multiple (fourfold) twinning on {100} facets (Fig. 7, d).

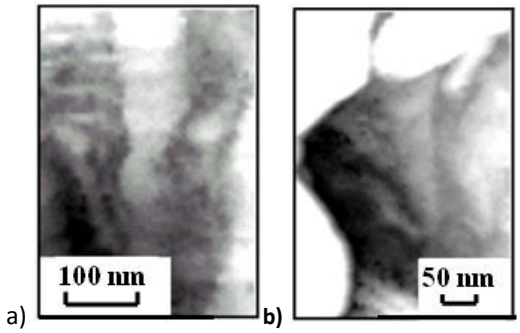

ISSN: 0975-8585

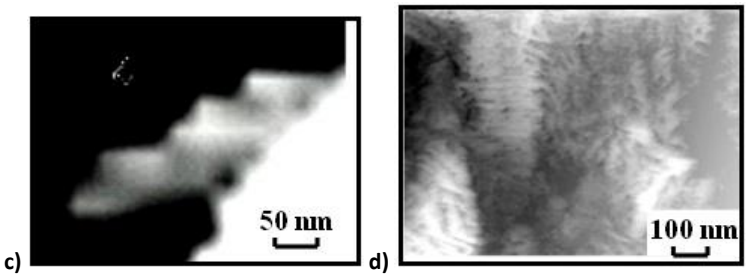

c) d)

Figure 7: Micrograph of the surface of $Ti_{1-x}Al_xN$ film at the stage of: formation of the primary axial <100> texture (*a*), geometric selection (*b*), formation of the secondary cone <110> texture on the axial <100> texture (*c*); multiple twinning on {100} facet (*d*)

(5) –Formation of the primary non-equilibrium polycrystalline $Ti_{1-x}Al_xN$ film with nondense structure (T_s/T_m = 0.205…0.22, $V_{heat.}$= 4.0 K/min). At the initial stage of the recrystallization, only primary non-equilibrium nondense structures form on the surface of $Ti_{1-x}Al_xN$ film, which are characterized by the columnar morphology. An enhanced thin structure with irregular crystallites direction is divided into domains 1…5 nm in size by a network of parallel microcavities (Fig. 8, *a*).

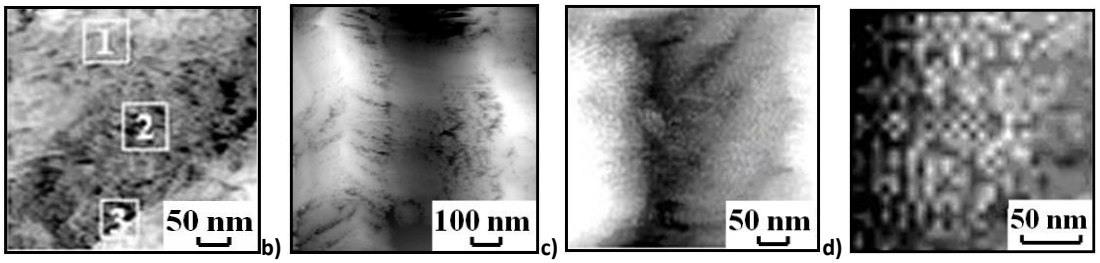

a) b) c) d)

Figure 8: Micrograph of the surface of $Ti_{1-x}Al_xN$ film at the stage of: formation of the primary non-equilibrium polycrystalline $Ti_{1-x}Al_xN$ film (*a*) and texturizing of crystallites (*b*, *c*) with the evolution of superficial fractal structure (*d*)

(6)–Texturizing of crystallites into plate-like buildups (T_s/T_m to 0.22…0.23, $V_{heat.}$= 4.0 K/min). The film thickness increase from 1.6 to 5.9 μm is accompanied by the specific texturizing of crystallites into plate-like buildups. The cross-section of pyramid-like crystallites with pseudo-hexagonal supports is 20 nm. These crystallites are combined into assemblies without sacrificing the boundaries coherence (nanoparticles), though the assemblies are combined into macrosystems in breach of boundaries continuity and coherence (Fig. 8, *b*, *c*). This phenomenon is indicative of the fact that the aggregation of crystallites results from a duration increase of substrate thermal influence. If formation conditions change, columnar substructures form not necessarily at initial stages. It is found that the surface roughness of $Ti_{1-x}Al_xN$ film changed into the fractal geometry (Fig. 8, *d*).The last thing is no surprise, since the formation of ion-plasma films generally takes place in the region of thermodynamic or kinetic instability of the film formation and is indicative of its complex hierarchy.

Further investigations showed, in the range under discussion T_s/T_m =0.15…0.23 and $V_{heat.}$= 1.9…4 K/min, the film structure formation runs not in equilibrium and completes with formation of nondense polycrystalline$Ti_{1-x}Al_xN$ films with columnar structure.

The increase of $V_{heat.}$ to 6 K/min, after the stage *4*, was found to provide a decrease of crystallites disorientation, their nanostructuring and progress of the stage (*5*) - formation of solid nanostructured $Ti_{1-x}Al_xN$ film with homogenous structure in the direction of formation* (Fig. 9).

An increase of thermal influence on the substrate in the deposition of $Ti_{1-x}Al_xN$ film provides an improvement of nucleation due to an increase of seeds number, a diameter decrease of primary crystallites to 5 nm, a restriction of their coarsening during combination and geometric selection, a stabilization of structuring of the nanostructured $Ti_{1-x}Al_xN$ film and a directional change in the preferred crystal-lattice orientation of crystallites.

ISSN: 0975-8585

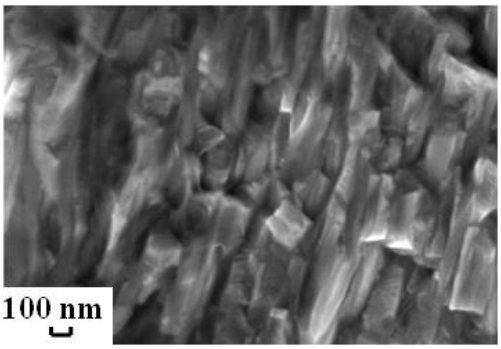

Figure 9: Micrograph of the fracture of $Ti_{1-x}Al_xN$ film at the stage of: formation of the nanostructured $Ti_{1-x}Al_xN$ film with preferred crystallites orientation

The intensity of reflections, normalized to the film thickness (h), was found to be extremum for films under discussion (103) $Ti_3Al_2N_2$ (I_{103}) (Fig. 10). I_{103}/hat T_s/T_m> 0.20 decreases sharply. The texturizing was previously found to be dominant in the range of temperatures T_s/T_m =0.17…0.20, when the film temperature increases in future–nanostructuring of crystallites and formation of the solid polycrystalline film.

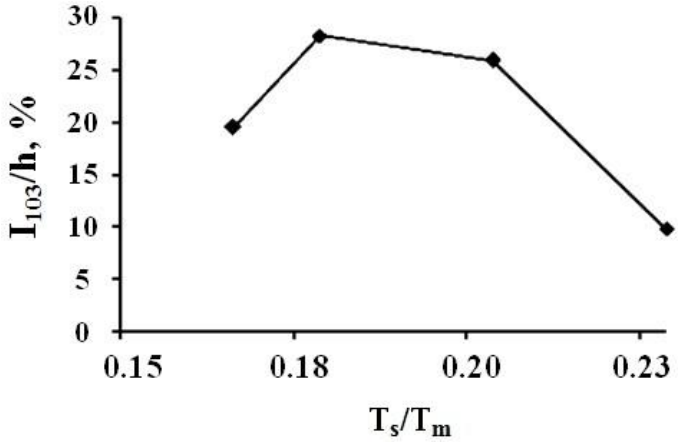

Figure 10: A relation of reflections intensities (103)$Ti_3Al_2N_2$, normalized to the film thickness from T_s/T_m

The developed structure zone model is given in Fig. 11.

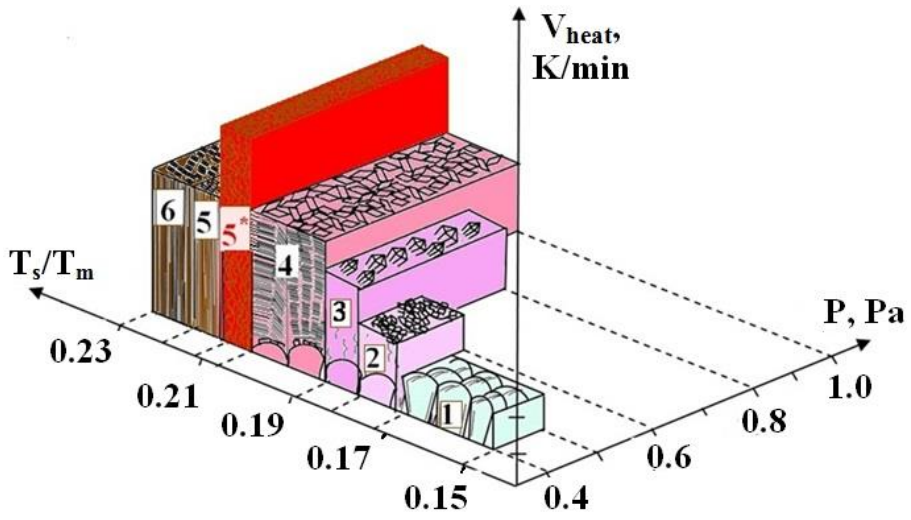

Figure 11: Model of Kameneva (2013): cathodic arc evaporation

SUMMARY

Using the low-resolution microscopy, Movchan and Demchishin developed SZM for thick single-phase films formed by electron-beam evaporation. In the zone 1, the diameter of hemispheres of dome-shaped globules increases with T_s/T_m. Grovernor etc., for thick and thin metal films, as well as for those formed by electron-beam evaporation, gave a guess that regardless the substrate temperature, small equiaxial grains are always the original film structure. At $T_s/T_m<0.3$, grain sizes are in a relatively narrow range due to the fact that phase transformations result from athermic processes in many systems, and diffusion effects are negligible.

During thermal evaporation in the zone 1 and under, a dense structure with a fine fiber texture develops. The density of saturation nucleation determines initial planar grain sizes. The mobility of adatoms is low, and columns keep the random nuclei orientation, as predicted in ballistic models. Columns are generally not singular grains; they are composed of small more equiaxial grains or may be fully amorphous. The surface roughness changes in fractal geometry, which, due to the wide angular distribution of deposition flow, atomic shadowing and limited surface diffusion, leads to an extensive porosity.

In case of the anodic arc evaporation at $T_s/T_m< 0.3$ and average ion energy per atom $<E_i>$ above 1 eV/atom, the zone 1 was replaced by zone M with a dense metastable structure in Mausbach's model. The grain growth in zone M is athermic with an average grain size of about 1 μm. With increasing $<E_i>$, the recrystallization time increases. The film metastability is related to point defects in its structure, which diffuse at room temperature due to their low activation energy.

The zone 1, compared to previous SZM, may be presented as an independent structure zone model. In the low-temperature range $0.15<T_s/T_m< 0.23$, the structure evolution of three-component thin polycrystalline films $Ti_{1-x}Al_xN$ and $Ti_xZr_{1-x}N$ with T_m ~ 4000 K was studied. Formation stages of $Ti_{1-x}Al_xN$ and $Ti_xZr_{1-x}N$ films during cathodic arc evaporation are determined, and a SZM of films as a function of T_s/T_m and V_{heat} is developed. It was shown that at $V_{heat.}\leq$ 4 K/min, the structure formation runs not in equilibrium and completes with a nondense polycrystalline film with a fractal surface structure. The increase of adatoms mobility, decrease of crystallites disorientation, their preferred orientation and formation of the solid nanostructured homogenous film in the direction of formation are enabled by the optimum film heating rate in the process of its deposition $V_{heat.}$= 6 K/min.

Regardless of evaporation method, regulation and control of the structure formation in the zone 1 is possible through the increase of average ion energy per atom and film heating rate.

ACKNOWLEDGMENTS

The research was financially supported by the Ministry of Education and Science of Russian Federation, research project №11.1913.2014/К – "Research of physico-chemical deposition processes of diamond films on ceramic materials"

REFERENCES

[1] Movchan BA, Demchishin AV. Phys. of Metals and Metallography (USSR) 1969;28:83.
[2] Batalin GI, Kushkov VD, Kachur AV, Grechanuk NI. The structure of the vacuum condensates stabilized zirconia // Dokl. Ukrainian Academy of Sciences. Ser. A. 1983;3:82–84.
[3] Bochkarev AA, Poluakova VI. The formation of micro- and nano-dispersed systems, 2010;pp. 468.
[4] Paton BE, Kishkin CT, Stroganov GB. Heat resistance of nickel alloys and cast their protection against oxidation, 1987;pp.256.
[5] Thornton JA. Influence of apparatus geometry and deposition conditions on the structure and topography // J. Vac. Sc. and Tech. – 1974; 11:666–670.
[6] Palatnik LS, Fuks MY, Kosevich BM. The mechanism of formation and substructure condensed films, 1972;pp.320.
[7] Chopra K.L., Kandlett M.R. Influence of deposition parameters on the coalescence stage of growth of metal films// J. Applied Physic. 1968;39(3):1874–1881.

[8] Eisner BA. Scientific principles of the deposition of multicomponent coatings of different functional purpose by vacuum electric-arc method: dis. … of D.Sc. in engineering / Belarusian State University. Minsk, 1993;pp.463.
[9] Grovenor CRM, Hentzell HTG, Smith DA. The development of grain structure during growth of metallic films // Acta Metallogr. 1984;32:773–781.
[10] Thornton J. High-rate thick-film growth // Annu. Rev. Mater. Sci. 1977;7:239–260.
[11] Messier R., Giri A.P., Roy R.A. Revised structure zone model for thin film physical structure // J. Vac. Sci. Technol. 1984, A2, 500–503.
[12] Microstructure in Tungsten Sputtered Thin Films / A.M. Haghiri-Gosnet, F.R. Lodan, C. Mayeux, H. Larnois // J. Vac. Sci. Technol. 1989, A7, 2663–2669.
[13] Hentzell H.T.G., Anderson B., Karlsson S.E. Grain size and growth of Ni-Rich Ni-Al alloy films // Acta Metall. 1983, 31, 2103–2111.
[14] Barna P.B. The evaluation of the technology for depositing NiCr resistive films // Proc. 9th Int. Vacuum Cong. Eds. de Segovia. 1983, 379–382.
[15] Sürgers C., Strunk C., Löhneysen H.V. Effect of substrate temperature on the microstructure of thin niobium films // Thin Solid Films. 1994, 239, 51–56.
[16] Misják Fanni. Szerkezetkialakulás Többfázisú Vékonyrétegekben: Doktori értekezés. Budapest: Műszaki Fizikai és anyagtudományi kutatóintézet, 2009. 117.
[17] Wen-Jun Chou. Processing and Properties of Metal Nitride Thin Films Deposited by PVD Methods: PhD thesis. The Republic of China: National Tsing Hua University, 1992;pp.177.
[18] Wang L. Investigation of the mechanical behavior of freestanding polycrystalline gold films deposited by evaporation and sputtering methods: Doctoral dissertation. – Auburn, Alabama, Auburn University, 2007;pp.195.
[19] Adamik M, Barna PB. Role of underlayers in the development of evolutionary texture in polycrystalline thin films // J. Surf. and Coat. Tech. 1996;80(1–2):109–112.
[20] Microstructural evolution during film growth / I. Petrov, P.B. Barna, L. Hultman, J.E. Greene // J. of Vacuum Science and Technology. 2003;21(5): 117–128.
[21] Rauschenbach B., Gerlach J.W. Texture development in titanium nitride films grown by low-energy ion assisted deposition // Cryst. Res. Technol. 2000;35:675–688.
[22] Schneider JM, Sproul WD, Matthews A. Magnetron sputtering Reactive ionized magnetron sputtering of crystalline alumina coatings // Surf. Coat. Technol. 1998;98:1473–1476.
[23] Mausbach M, Microstructure of copper films condensed from a copper plasma with ion energies between 2 and 150 eV // Surf. Coat. Technol. 1995;74-75:264-272.
[24] Kameneva AL, V.I. Kichigin, T.O. Soshina, V.V. Karmanov. Using $Ti_{1-x}Al_xN$ coating to enhance corrosion resistance of tool steel in sodium chloride solution, Research Journal of Pharmaceutical, Biological and Chemical Sciences, 2014;5(5): 1148-1156.
[25] Kameneva AL, V.V. Karmanov, I.V. Dombrovsky. Physical and mechanical properties of $Ti_{1-x}Al_xN$ thin films prepared by different ion-plasma methods, Research Journal of Pharmaceutical, Biological and Chemical Sciences, 2014;5(6):762-771.
[26] Kameneva AL. The influence of aluminum on the texture, microstructure, physical, mechanical and tribological properties of $Ti_{1-x}Al_xN$ thin films, Research Journal of Pharmaceutical, Biological and Chemical Sciences, 2014;5(6):965-975.
[27] Kameneva AL. The influence of TiN, ZrN and $Ti_xZr_{1-x}N$ layers of anti-friction multi-layer coatings on corrosion resistance of hard alloy in sodium hydroxide solution, Research Journal of Pharmaceutical, Biological and Chemical Sciences, 2015;6(1):1381-1391.
[28] Kameneva AL. Forming Stages of Polycrystalline Thin Films Depending on the Nitrogen Concentration in Mixed Gas // Journal of Materials Sciences and Applications. 2011;2(1):6–13.
[29] Kameneva AL, Soshina TO, Guselnikova LN. An influence of a substrate voltage bias and temperature conditions on structure and phase modification in single-component ion-plasmas' films // Journal of Surface Science and Nanotechnology. 2011;9(11):34–39.
[30] Kameneva AL, Soshina TO, Guselnikova LN. Forming and nanostructuring processes of film with main hexagonal phase $TiN_{0,3}$ during arc spraying // Journal of Biophysical Chemistry. 2011;2(1):26–31.